Friction Anisotropy of the Surface of Organic Crystals and Its Impact on Scanning Force Microscopy

M. Campione*

Department of Geological Sciences and Geotechnologies, Università degli Studi di Milano Bicocca, Piazza della Scienza 4, I-20126 Milan, Italy

E. Fumagalli

Department of Materials Science, Università degli Studi di Milano Bicocca, Via R. Cozzi 53,I-20125 Milan, Italy

(Received 19 July 2010; published 12 October 2010)

The transverse component of the friction forces acting on the tip of an atomic force microscope scanning on the surface of an organic crystal was monitored as a function of the scan direction. The relation between friction and the crystallographic system is disclosed, revealing that the symmetry of the friction phenomenon is dictated by the direction of the prominent corrugations of the crystal surface. It is also illustrated that molecular-resolution images can be collected through the monitoring of the motion of the tip in a transverse direction with respect to the scan direction.

DOI: 10.1103/PhysRevLett.105.166103 PACS numbers: 68.35.Af, 07.79.Sp, 61.66.Hq, 68.37.Ps

Among scanning probe microscopies, atomic force microscopy (AFM) represents the benchmark technique for the topographical characterization of the surface of both conductive and nonconductive solids. A micrometric tip mounted on a cantilever is scanned over the sample surface thanks to piezoelectric actuators; the interaction of the scanning tip with the sample causes a perturbation of the cantilever static or dynamic state that is usually monitored by laser beam deflection. This experimental configuration has been demonstrated to be sensitive to surface topography fluctuations down to the nanoscale, allowing surface structure characterization [1,2]. Monitoring of cantilever vertical deflection is the simplest way for collecting topographical images, in the so-called constant height operation mode. By the use of a feedback loop, scanning can be performed in constant force mode and the image can be reconstructed from the piezoelectric movements in vertical direction (height image). It has also been shown that the cantilever torsion resulting from frictional forces between tip and surface allows the imaging of atomic-scale corrugations thanks to its sensitivity to the stick-slip motion of the scanning tip [3]. This is often referred to as lateral force microscopy (LFM) and, operatively, it requires one to set the fast-scan direction orthogonal to the cantilever axis. The torsion signal may also be collected by setting the fast-scan direction parallel to the cantilever axis. In this case the image contrast reflects differences in azimuthal orientation of crystalline domains [4,5]. Recently, this imaging mode has been referred to as transverse shear microscopy (TSM) [6], and it has been successfully employed for revealing the grain boundary network of pentacene monolayers on silicon oxide [6–8]. By using pentacene crystals, it was demonstrated how the torsion signal shows a periodic dependence on the angle between the scan direction and a crystallographic axis of the crystal surface. This periodic dependence can be exploited for (not univocally) determining the orientation of the crystal from the quantitative analysis of the hysteresis of the torsion signal. For pentacene, a period of π rad of the TSM signal was observed, zeroing along two directions coincident with the primitive crystallographic directions of the surface. Furthermore, the TSM signal revealed significant differences of its dependence on scan velocity and temperature with respect to the lateral force signal. These findings were considered consistent with a linear anisotropic elastic response of the surface consequent to a uniaxial stress applied by the scanning tip [9].

In this Letter, we extend the investigation of the TSM response to the surface of the organic crystal potassium hydrogen phthalate (KAP), for which, differently from pentacene, elastic coefficients are already known [10], then allow a direct comparison between the experimental TSM signal and that predicted by the elastic model. We find that the TSM signal as a function of scan angle zeros along six directions separated by 30° ca. one another, reflecting a pseudohexagonal symmetry. This result is demonstrated to be fully inconsistent with the in-plane elastic response of the crystal. Rather, the TSM signal arises from nonlinear effects related to the anisotropic friction, having a clear relation with surface crystallography. Finally, being certain of the frictional origin of the TSM signal, by analyzing the torsion signal during scanning at nanoscopic scales, an atomically modulated transverse tip motion is revealed, which can be exploited for collecting high quality molecular-resolution images.

KAP is a commercially available lamellar organic salt, which crystallizes from aqueous solution in an orthorhombic form (space group $Pca2_1$) with unit cell parameters $a = 9.61$ Å, $b = 13.33$ Å, $c = 6.48$ Å [11] [Fig. 1(a)].

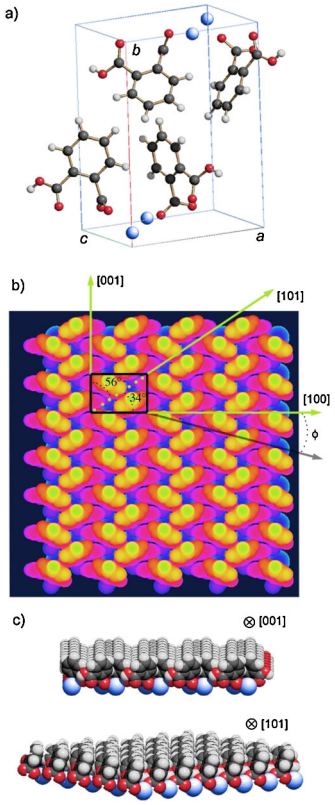

FIG. 1 (color online). (a) Crystal structure of KAP [gray (large dark balls): C atoms; red (small dark balls): O atoms and ions; blue (large bright balls): K ions; white (small bright balls): H atoms] and unit cell axes. (b) Representation with a depth-dependent color scale of the cleavage surface of KAP; the surface unit cell is indicated by a black rectangle; significative crystallographic directions are indicated by green (bright) arrows; ϕ is the angle between KAP[100] and the scan direction (black arrow). (c) Structural models of the cleavage surface of KAP as viewed along the [001] and [101] directions, pointing out the main surface corrugations.

The cleavage surface of KAP is parallel to the (010) plane and is lined up with hydrogen atoms bonded to the phenyl rings [Figs. 1(a) and 1(c)]. A 100 μm-thick slice of KAP was freshly cleaved with a razor blade and fixed with tape on a rotating holder with a goniometric scale (precision $\pm 2°$). Using a Nanoscope V MultiMode AFM (Veeco) with a single-beam silicon nitride tip (force constant 0.7 N/m) we collected the TSM signal of the cantilever (trace horizontal deflection minus retrace horizontal deflection) along crystallographic directions forming an angle ϕ to KAP[100], under an applied load of 35 nN and at a scan velocity of 9 μm/s. The results are reported in Fig. 2. The torsion signal presents the following relevant features: (i) it has a period of π rad, (ii) within a period, it zeros seven times, approximately every 30°, (iii) the changes in sign occur abruptly, especially at 90° and 270°, resembling a discontinuity. The experimental TSM signal is superimposed in Fig. 2(a) with that predicted by the elastic model proposed by Kalihari *et al.* [9] (TSM_E).

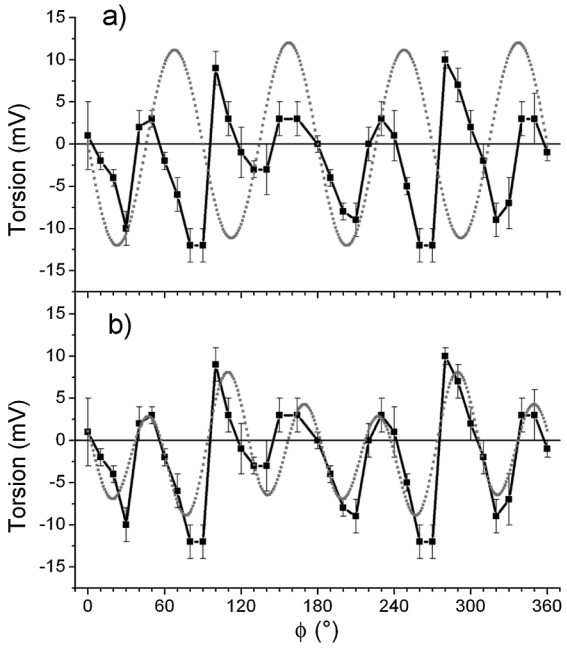

FIG. 2. Solid line: experimental TSM signal collected on the KAP(010) surface as a function of the angle ϕ (10° steps). Dotted line: (a) TSM signal calculated from the in-plane elastic constants of KAP [10] using Eq. (1), (b) TSM signal calculated from a nonlinear model of anisotropic friction with six principal directions and constant friction coefficients.

For this model, we have to consider the xz-plane elastic constants C_{ij} of KAP, which contribute to the TSM signal in accordance with the following equation:

$$\begin{aligned}\mathrm{TSM}_E \propto\ & C_{11}(-\cos^3\phi\sin\phi) + C_{33}(\sin^3\phi\cos\phi) \\ & + C_{55}(2\cos^3\phi\sin\phi - 2\sin^3\phi\cos\phi) \\ & + C_{13}(\cos^3\phi\sin\phi - \sin^3\phi\cos\phi) \\ & + C_{35}(3\sin^2\phi\cos^2\phi - \sin^4\phi) \\ & + C_{15}(\cos^4\phi - 3\sin^2\phi\cos^2\phi), \end{aligned} \tag{1}$$

where $C_{11} = 20.1$ GPa, $C_{33} = 19.6$ GPa, $C_{55} = 5.2$ GPa, $C_{13} = 0.2$ GPa, $C_{35} = 0$, $C_{15} = 0$ [10]. The TSM_E curve reported in Fig. 2(a) presents the following features: (i) it has a period of π rad, (ii) within a period, it zeros only five times, approximately every 45°, (iii) the changes in sign occur smoothly. Among them, point (ii) is the most important discrepancy between the model and the experiment, and it is sufficient to rule out any influence of surface elasticity on the detected torsion signal. Assuming heuristically that the TSM signal originates from friction phenomena [4], the directions along which the torsion signal is zero are referred to as principal direction of friction. In the case of KAP(010), we identify six principal directions. In the framework of models of anisotropic friction [12–14], the friction force vector $\mathbf{t}$ can be conveniently expressed as a polynomial function of the form

$$\boldsymbol{t} = -N(\mathbf{B}_1\boldsymbol{v} + \mathbf{B}_2\boldsymbol{v}^3 + \cdots + \mathbf{B}_n\boldsymbol{v}^{2n-1}), \quad (2)$$

where N is the normal force, $\mathbf{B}_i$ are tensors of order 2_i, $\boldsymbol{v}$ is the slip velocity unit vector ($[v] = [\cos\phi, \sin\phi]$), and the exponent of $\boldsymbol{v}$ denotes a tensor product. Six principal directions of friction can be admitted only by considering at least the first three terms of the polynomial. The TSM signal is assumed to be proportional to the transverse component of the friction vector, i.e., to the projection of $\mathbf{t}$ along the direction of the unit vector orthogonal to the slip direction $[v^\perp] = [-\sin\phi, \cos\phi]$:

$$\mathrm{TSM}_F \propto \boldsymbol{t}\cdot\boldsymbol{v}^\perp = -N(\mathbf{B}_1\boldsymbol{v} + \mathbf{B}_2\boldsymbol{v}^3 + \mathbf{B}_3\boldsymbol{v}^5)\cdot\boldsymbol{v}^\perp. \quad (3)$$

By considering the tensors $\mathbf{B}_1$ and $\mathbf{B}_2$ as spherical, the development of the previous equation brings us to the following formula:

$$\begin{aligned}\mathrm{TSM}_F \propto -N(&\tilde{B}_1\cos^6\phi + \tilde{B}_2\cos^5\phi\sin\phi \\ &+ \tilde{B}_3\cos^4\phi\sin^2\phi + \tilde{B}_4\cos^3\phi\sin^3\phi \\ &+ \tilde{B}_5\cos^2\phi\sin^4\phi + \tilde{B}_6\cos\phi\sin^5\phi + \tilde{B}_7\sin^6\phi),\end{aligned} \quad (4)$$

where $\tilde{B}_1 = B^{211111}$, $\tilde{B}_7 = B^{122222}$, and the other tilded coefficients are simple sums and differences of the other 62 coefficients of the sixth-order tensor $\mathbf{B}_3$. The best fit of the experimental TSM curve using Eq. (4) is reported in Fig. 2(b). This result has been obtained imposing no constraint on $\tilde{B}_i$ coefficients and using as initial values those corresponding to a system with hexagonal symmetry ($\tilde{B}_1 = 0, \tilde{B}_2 = \tilde{B}_6, \tilde{B}_3 = 0, \tilde{B}_4 = -3.34\tilde{B}_6, \tilde{B}_5 = 0, \tilde{B}_7 = 0$). The calculated best-fit values are $\tilde{B}_1 \cong 0$, $\tilde{B}_2 \cong 0.7$, $\tilde{B}_3 \cong 0.9\tilde{B}_6$, $\tilde{B}_4 \cong -2.4\tilde{B}_6$, $\tilde{B}_5 \cong -0.7\tilde{B}_6$, $\tilde{B}_7 \cong 0$. The adequacy of a nonlinear model of anisotropic friction is apparent from the close agreement between experimental and fitted curves reported in Fig. 2(b). However, the definitive proof of the friction origin of the TSM signal is given by the position of the principal directions. Best-fit principal directions are found at $\phi = 2°, 37°, 57°, 94°, 127°, 157°$. Within the experimental uncertainty of the sample azimuth, these directions correspond to the following crystallographic directions on the KAP(010) surface (Fig. 1): orthogonal to [001] (0°), [$\bar{1}$01] (34°), orthogonal to [101] (56°), [001] (90°), orthogonal to [$\bar{1}$01] (124°), [101] (146°). In other terms, the transverse component of friction is zero when the tip is scanned parallelly and perpendicularly to the ⟨001⟩ and ⟨101⟩ crystallographic directions.

The role of these directions on the friction phenomenon is readily understood by an inspection of the corrugation of the KAP(010) surface. Indeed, as can be observed in Fig. 1(c), the ⟨001⟩ and ⟨101⟩ directions individuate nanoscopic parallel furrows with spacing of 0.96 and 0.54 nm, respectively, formed by the arrangement of prominent phenyl rings. These furrows act as rails for the scanning tip, forcing it to deviate its trajectory from that imposed by the scan direction: as a result, the cantilever undergoes a torque, giving rise to the TSM signal. The abrupt sign variations detected at $\phi = 90°$ and $\phi = 270°$ can be related to the morphology of the furrows. Indeed, the larger spacing of ⟨001⟩-oriented grooves with respect to ⟨101⟩ ones makes the former more effective as lateral barriers to the tip motion [see Figs. 1(b) and 1(c)]. Then, slight rotations from 90° or 270° cause large transverse forces. Notwithstanding the simplicity of this scenario, the presence of three cooperating directions of strong corrugation arranged in a pseudo-hexagonal fashion gives rise to a marked nonlinear effect, which is difficult to assume *a priori*.

In light of the previous arguments, the results obtained on pentacene crystals described in Ref. [9] can be reinterpreted in relation to linear models of friction anisotropy. It was found that the TSM signal went to zero along two mutually orthogonal (principal) directions coinciding with the primitive crystallographic directions of the crystal surface. This corresponds to orthotropic friction, which is described by a diagonal second-order tensor $\mathbf{B}_1$ with two independent coefficients. Following the steps bringing us to Eq. (4), the TSM signal of an orthotropic surface results in $\mathrm{TSM} \propto N(B^{22} - B^{11})(\sin 2\phi)$, which perfectly fits the experimental trend obtained for pentacene.

We consider it worth noting that the same conclusion can be drawn using a simple mechanical model of a rigid textured surface with parallel trenches of nanoscopic spacing. When the tip is scanned at an angle ϕ to the axes of trenches, considering the action of each trench as a rigid obstacle (wall) pushing against the tip, it is subjected to a drag force of transverse component proportional to $\sin 2\phi$. The effect of the presence of parallel trenches along multiple directions (corrugations, in the framework of the surface of crystals) cannot be deduced by a simple linear combination, which would always bring us to a force proportional to $\sin 2\phi$; rather, it gives rise to marked nonlinearities which, as in the case studied, are well described by a polynomial function of the scan velocity vector [Eq. (2)]. In this respect, the significant differences, investigated by Kalihari *et al.* [9], of the dependence of the TSM signal on scan velocity and temperature with respect to the lateral force signal, can be related to the different nature of the transverse and longitudinal components of the friction force. Namely, the TSM signal originates from a constraint reaction due to the inherently structured surface of organic crystals; this reaction can reasonably be considered independent of temperature and scan velocity. On the contrary, the LFM signal is strictly connected to the instantaneous formation and breaking of molecular bonds. This latter is a thermally activated process and it is responsible for a logarithmic dependence of friction on scan velocity [15]. As a final remark, two points must be considered, accounting for the quantitative discrepancy between calculated and experimental data [see Fig. 2(b)]. (i) The coefficients of the tensors appearing in Eq. (2) are in general periodic

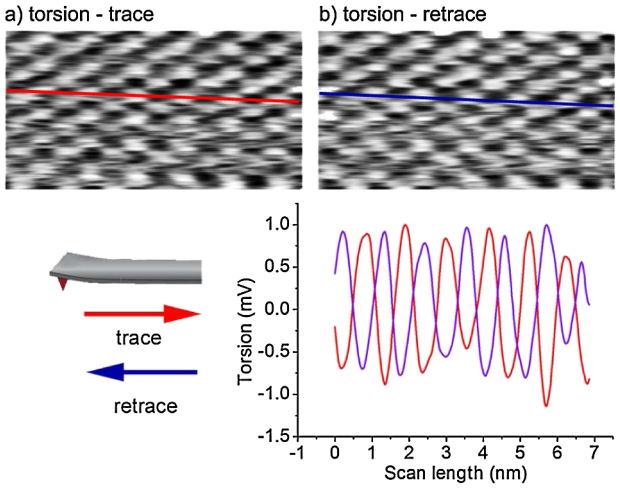

FIG. 3 (color online). Molecular-scale TSM images (7×3.5 nm^2) collected on the KAP(010) surface at $\phi = 345°$. The cross-sectional profiles taken along the gray (red and blue) lines are reported in the graph (offset has been subtracted), showing the periodicity corresponding to the (100) corrugation and the inverse relation between the trace and retrace signal, respectively.

functions of the angle ϕ, whereas we assumed them as constant, and (ii) friction is always the result of the composition of frictional anisotropies coming from two different contacting surfaces: in our case, the surface of the organic crystal and that of the AFM tip. Eventual anisotropies of the tip surface, which can be considered relatively weak, may influence the dependence of the TSM signal on the scan angle, and this accounts for the variations observable by repeating measurements with different tips.

As a final step of our investigation, we studied the variations of the TSM signal while scanning on the KAP (010) surface at nanoscopic scales. By setting the ϕ parameter at values where the TSM signal reaches its relative maxima, we realized that the contrast in TSM images reproduced the surface corrugation of the sample [compare Fig. 3 with Fig. 1(b)]. This result demonstrates that the cantilever is not stationarily twisted, but its torsion varies with a periodicity given by the position of protruding superficial H atoms. This is surprisingly equivalent to the atomically modulated sliding attainable in the LFM modality [16]; however, in TSM the direction of periodic motion of the tip is orthogonal to the scan axis. In Fig. 3 the surface lattice of KAP(010) with its rectangular unit cell is easily resolved by scanning at $\phi = 345°$, an angle corresponding to a relative maximum of the TSM signal. Two cross-sectional profiles taken along the same scan line but with opposite paths are reported below Fig. 3(b), showing the centrosymmetry of the signal.

To conclude, using KAP as a paradigmatic system, we unraveled the physical nature of the torsion signal detected by AFM when the tip is scanned parallelly to the cantilever axis on crystalline organic surfaces. This signal stems from the friction anisotropy conferred by pronounced corrugations typical of the surface of organic crystals. The symmetry of the friction phenomenon has been observed to reproduce that given by the arrangement of prominent surface corrugations, consisting in parallel furrows running along low Miller index directions. As a general guideline emerging from our study, the axes of the furrows correspond to principal directions of friction, then, whenever the tip is scanned along these directions, the TSM signal zeros. The friction nature of this signal enables us to exploit the transverse motion of the AFM tip for collecting molecular-resolution images with high quality, representing a new modality of AFM high-resolution imaging.

Paolo Campiglio is kindly acknowledged for realizing for the first time the sensitivity of the TSM signal to surface corrugations. This work was supported by Fondazione Cariplo (Grant No. 2007/5205).

*marcello.campione@unimib.it

[1] G. Binnig, C. F. Quate, and C. Gerber, Phys. Rev. Lett. **56**, 930 (1986).
[2] G. Binnig, C. Gerber, E. Stoll, T. Albrecht, and C. Quate, Europhys. Lett. **3**, 1281 (1987).
[3] C. M. Mate, G. M. McClelland, R. Erlandsson, and S. Chiang, Phys. Rev. Lett. **59**, 1942 (1987).
[4] J. Last and M. Ward, Adv. Mater. **8**, 730 (1996).
[5] R. Carpick and M. Salmeron, Chem. Rev. **97**, 1163 (1997).
[6] V. Kalihari, E. Tadmor, G. Haugstad, and C. Frisbie, Adv. Mater. **20**, 4033 (2008).
[7] K. Puntambekar, J. Dong, G. Haugstad, and C. Frisbie, Adv. Funct. Mater. **16**, 879 (2006).
[8] J. Zhang, J. Rabe, and N. Koch, Adv. Mater. **20**, 3254 (2008).
[9] V. Kalihari, G. Haugstad, and C. D. Frisbie, Phys. Rev. Lett. **104**, 086102 (2010).
[10] A. V. Alex and J. Philip, J. Appl. Phys. **88**, 2349 (2000).
[11] T. Eremina, N. Furmanova, L. Malakhova, T. Okhrimenko, and V. Kuznetsov, Crystallogr. Rep. **38**, 236 (1993).
[12] A. Zmitrowicz, Int. J. Solids Struct. **25**, 837 (1989).
[13] A. Zmitrowicz, Int. J. Solids Struct. **29**, 3025 (1992).
[14] A. Zmitrowicz, Int. J. Solids Struct. **29**, 3045 (1992).
[15] E. Riedo, E. Gnecco, R. Bennewitz, E. Meyer, and H. Brune, Phys. Rev. Lett. **91**, 084502 (2003).
[16] R. M. Overney, H. Takano, M. Fujihira, W. Paulus, and H. Ringsdorf, Phys. Rev. Lett. **72**, 3546 (1994).